ARCHIVES OF ACOUSTICS
22, 2, 169–177 (1997)

SINGULARITIES OF THE PLANAR GREEN FUNCTION IN THE SPECTRAL DOMAIN

W. LAPRUS and E. DANICKI

Institute of Fundamental Technological Research,
Polish Academy of Sciences
(00-049 Warszawa, ul. Świętokrzyska 21)

The surface acoustic wave amplitudes at the boundary of a piezoelectric half-space satisfy a matrix relation which is characteristic of the medium. The elements of the matrix are functions of slowness. In the paper, the singularities of the matrix are investigated at cutoff points of bulk waves. An approximated formula is derived for the matrix in the neighborhood of the greatest cutoff point, which also takes into account the singularity related to the Rayleigh wave. The results of numerical calculations are presented for several piezoelectrics.

1. Introduction

The INGEBRIGTSEN effective permittivity [1, 2] of a piezoelectric half-space, a function of slowness r, is an approximation of the exact effective permittivity $Y(r)$ in the vicinity of the singular point equal to the Rayleigh wave slowness. The counterpart of $Y(r)$ in the space domain, i.e. the Fourier transform of $Y(r)$, is a Green function defined at the boundary of the piezoelectric half-space. The Green integral formula applied to the electric potential at the boundary gives the surface electric charge density.

In the special case of SH waves, the Ingebrigtsen approximation has been improved by including contributions from bulk waves [3]. Since only one component of the particle displacement vector is different from zero, the contributions can be found in an analytic way.

We consider the general case when all the three components of the particle displacement vector may be different from zero, so that numerical calculations are necessary. For this purpose we employ the ADLER form of the field equations [4], which proves to be very useful in the analysis of piezoelectric interfacial waves [5, 6, 7].

We are interested in the approximation of the function $Z(r) = C/Y(r)$ (C is a constant) in the vicinity of the cutoff point of bulk waves; this is a branch point of $Z(r)$ in the complex plane of r. It is shown that the behavior of the function $Z(r)$ near the cutoff point depends on the shape of the corresponding slowness curve at that point.

Starting from the derived approximation of $Z(r)$, we take into account the Rayleigh wave singularity, and find an approximated formula for the function $Z(r)$ that is valid

in the whole range of r. The formula is verified by comparison with the exact function $Z(r)$ calculated numerically.

2. Function $Z(r)$

Let us consider a homogeneous piezoelectric medium and a system of coordinates (x, y, z). The plane $z = 0$ divides the medium into two half-spaces: the upper (for $z > 0$) and the lower (for $z < 0$). We assume that the field is independent of y, and that the time and space dependence is given by the factor $\exp(j\omega t - j\omega r x - j\omega s z)$.

The field equations can be reduced to the system of eight linear algebraic equations, as described in Ref. [7]. Let $i, j = 1, 2, 3$ and $(x_i) = (x, y, z)$. The following field variables will be used: particle displacement u_i, electric potential ϕ, surface force $T_i = T_{3i}$ (where T_{ij} is the stress tensor), and normal component D_3 of the electric displacement D_i. We have

$$H_{KL}(r) F_L = q F_K \,, \tag{2.1}$$

where $K, L = 1, \ldots, 8$, $(F_K) = (j\omega r u_i, j\omega r \phi, T_i, D_3)$, and $q = s/r$. For real r, which we assume, the matrix H_{KL} is real and non-symmetric. It depends on material constants (see Ref. [7]).

The summation convention is adopted throughout the paper: summation is performed over repeated indices (within their range) except when they are enclosed in parentheses.

After solving the eigenvalue problem defined by Eq. (2.1) we get eight eigenvectors $\tilde{F}_K^{(J)}(r)$ corresponding to eight eigenvalues $q^{(J)}(r)$ for $J = 1, \ldots, 8$. The J-th eigenwave has the form

$$F_K^{(J)} = \tilde{F}_K^{(J)} \exp(j\omega t - j\omega r(x + q^{(J)} z)). \tag{2.2}$$

The solution of the field equations is a linear combination of the eigenwaves.

The eigenvector $\tilde{F}_K^{(J)}$ will be called upper (lower) if $\operatorname{Im} q^{(J)} < 0$ ($\operatorname{Im} q^{(J)} > 0$) or, for $\operatorname{Im} q^{(J)} = 0$, if the z component of the real part of the Poynting vector is positive (negative). $\operatorname{Im} q^{(J)} \neq 0$ for $J = 1, \ldots, 8$ if $r > r_c$ where r_c is the cutoff slowness of bulk waves.

Since the surface wave field vanishes at infinity, and there is no energy flux to the boundary (no sources in the space), the solution F_K^+ of the field equations in the upper half-space consists of upper eigenwaves, and the solution F_K^- in the lower half-space consists of lower eigenwaves. At the plane $z = 0$, the complex amplitudes of the two solutions are

$$\tilde{F}_K^{\pm} = \sum_J^{\pm} C_J \tilde{F}_K^{(J)} \,, \tag{2.3}$$

where the plus (or minus) superscript of the sum symbol means that the summation is performed over J such that $\tilde{F}_K^{(J)}$ is an upper (or lower) eigenvector. The coefficients C_J are to be determined from boundary conditions.

The field equations can be solved in each half-space separately, provided appropriate boundary conditions are imposed at the plane $z = 0$. In general, all the boundary values $\tilde{F}_K^+$ (or $\tilde{F}_K^-$) should be given. However, we consider special solutions (surface waves),

and therefore the field variables satisfy some additional relation at the boundary of each piezoelectric half-space. Below, it will be shown that only four of the eight boundary values may be arbitrary.

Let $R_{KJ} = \widetilde{F}_K^{(J)}$. If we change the order of the columns of the matrix R_{KJ} so that the first four are upper eigenvectors and the last four are lower eigenvectors, then the matrix can be written in the form

$$(R_{KJ}) = \begin{bmatrix} R^+ & R^- \\ S^+ & S^- \end{bmatrix}, \tag{2.4}$$

where R^+, R^-, S^+, and S^- are 4×4 matrices. Denote by $L^\pm$ the inverses of the matrices $S^\pm$.

Using the notation $(\widetilde{F}_K^\pm) = (\widetilde{U}_L^\pm, \widetilde{T}_L^\pm)$ for $L = 1, \ldots, 4$, we rewrite Eq. (2.3) as

$$\widetilde{U}_K^\pm = R_{KJ}^\pm C_J^\pm, \qquad \widetilde{T}_K^\pm = S_{KJ}^\pm C_J^\pm \tag{2.5}$$

for $J, K = 1, \ldots, 4$, where C_J^+ and C_J^- are the coefficients of the upper and the lower eigenvectors in Eq. (2.3). From Eq. (2.5) we find $C_J^\pm = L_{JL}^\pm \widetilde{T}_L^\pm$, and then

$$\widetilde{U}_K^\pm = Z_{KL}^\pm \widetilde{T}_L^\pm, \tag{2.6}$$

where the matrix

$$Z_{KL}^\pm = R_{KJ}^\pm L_{JL}^\pm \tag{2.7}$$

depends on r.

Equation (2.6) is a fundamental relation in the problem of surface wave propagation. It should be satisfied by the field variables at the boundary of each piezoelectric half-space, irrespective of what boundary conditions are imposed there.

If the boundary of the piezoelectric half-space is traction-free then $\widetilde{T}_i^\pm = 0$ for $i = 1, 2, 3$. In this case, from Eq. (2.6) for $K = 4$, we have $\widetilde{U}_4^\pm = Z_{44}^\pm \widetilde{T}_4^\pm$ or

$$j\omega r \widetilde{\phi}^\pm = Z_{44}^\pm \widetilde{D}_3^\pm. \tag{2.8}$$

In the following, we shall be considering the function $Z(r) = -Z_{44}^-(r)$.

3. First order singularities

The function $Z(r)$ is infinite at the singular point $r_i > r_c$ related to the Rayleigh wave. Three other singular points for $r \leq r_c$ coincide with the cutoff points of the three slowness curves (in Fig. 1 the slowness curves have appendices for r greater than the corresponding cutoff points). The function $Z(r)$ is finite at these points (see Fig. 2) but its first derivative may be infinite; therefore, the corresponding singularities will be called first-order.

The idea of approximation of $Z(r)$ in the neighborhood of a cutoff point is based on the following observation. Consider the slowness curve with the cutoff point r_c. From Fig. 1 we see that for $r < r_c$ there exist two values of s, $s^\pm = q^{(\pm)}(r) r$ where $q^{(\pm)}(r)$

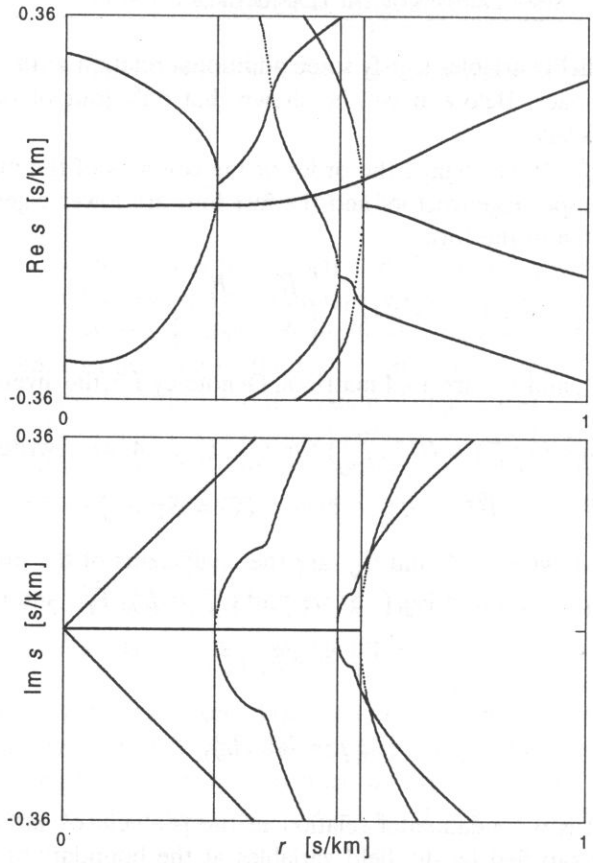

Fig. 1. The real and imaginary part of the slowness s for bismuth germanium oxide (Euler angles: 24°, 70°, 10°). The three vertical lines mark the cutoff points.

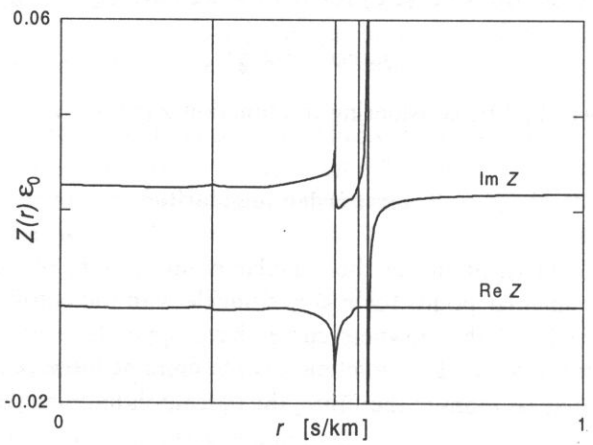

Fig. 2. The function $Z(r)$ for bismuth germanium oxide (Euler angles: 24°, 70°, 10°). The three vertical lines mark the cutoff points.

are the two real eigenvalues corresponding to the slowness curve. As $r \to r_c$, these two values converge to $s_c = q^{(0)} r_c$ where $q^{(0)} = q^{(\pm)}(r_c)$. The double real eigenvalue $q^{(0)}$ splits into a complex conjugate pair of eigenvalues for $r > r_c$.

It should be noted here that the matrix $H_{KL}(r)$ is defective for $r = r_c$: it has only seven independent eigenvectors. This can be shown by differentiation of the equality

$$\left(H_{KL} - q^{(J)} I_{KL}\right) \tilde{F}_L^{(J)} = 0 \tag{3.1}$$

(I_{KL} denotes the identity matrix) with respect to s along the slowness curve. In other words, the two eigenvectors $\tilde{F}_K^{(\pm)}$ corresponding to $q^{(\pm)}(r)$ converge to the eigenvector $\tilde{F}_K^{(0)}$ corresponding to the double eigenvalue $q^{(0)}$. The eigenvector $\tilde{F}_K^{(+)}$ is upper, and $\tilde{F}_K^{(-)}$ is lower in the neighborhood of r_c, because the real part of the Poynting vector is normal to the slowness curve.

The values $s^{\pm}$ are changing fast for $r \to r_c$ (the derivative of $s^{\pm}(r)$ tends to infinity), and so do the two corresponding eigenvalues and eigenvectors, while the other eigenvalues and eigenvectors are relatively constant. Thus, it suffices to take into account only the two eigenvectors $\tilde{F}_K^{(\pm)}$, to find the approximated formulae for them, and to calculate the function $Z(r)$ with the use of Eq. (2.7).

Suppose we know the function $s^{\pm}(r)$ in the neighborhood of r_c. Regarding the eigenvectors $\tilde{F}_K^{(\pm)}$ as functions of the variable s, we can write, separately for $s > s_c$ and $s < s_c$, the Taylor expansion

$$\tilde{F}_K^{(\pm)}(s^{\pm}) = \tilde{F}_K^{(0)} + \tilde{F}_K^{\bullet(0)} \Delta s^{\pm}, \tag{3.2}$$

where the higher-order terms are neglected; the dot denotes differentiation with respect to s, $\tilde{F}_K^{\bullet(0)}$ denotes the common limit of $\tilde{F}_K^{\bullet(\pm)}(s^{\pm})$ as $s^{\pm} \to s_c$, and $\Delta s^{\pm} = s^{\pm} - s_c$.

The slowness curve in the vicinity of r_c can be approximated by an algebraic curve of second order, such as circle or parabola. We get

$$\Delta s^{\pm} = \pm \alpha \rho(r), \qquad \rho(r) = \operatorname{sign}(r_c^2 - r^2)\sqrt{r_c^2 - r^2} \tag{3.3}$$

with $\alpha = (R_c/r_c)^{1/2}$ where R_c is the radius of curvature $R = (1 + (s')^2)^{3/2}/|s''|$ for $r = r_c$, and the prime denotes differentiation with respect to r. Since $s = qr$, we have

$$s' = q'r + q, \qquad s'' = q''r + 2q'. \tag{3.4}$$

The derivatives q' and q'' can be found by differentiation of Eq. (3.1) as follows.

Let $\tilde{E}_L^{(I)}$ be the left eigenvector corresponding to the eigenvalue $q^{(I)}$. We assume the normalization

$$\tilde{F}_L^{(J)} \tilde{F}_L^{(J)} = 1, \qquad \tilde{E}_L^{(I)} \tilde{F}_L^{(J)} = I_{IJ} \tag{3.5}$$

for every r, and introduce the symbols

$$Q_1^{(IJ)} = \tilde{E}_K^{(I)} H'_{KL} \tilde{F}_L^{(J)}, \qquad Q_2^{(IJ)} = \tilde{E}_K^{(I)} H''_{KL} \tilde{F}_L^{(J)}. \tag{3.6}$$

Differentiating Eq. (3.1) once and twice with respect to r, and multiplying the both sides by $\tilde{E}_L^{(I)}$ we obtain

$$q'^{(J)} = Q_1^{(JJ)}, \qquad q''^{(J)} = Q_2^{(JJ)} + 2 \sum_{I \neq J} C_{IJ} Q_1^{(JI)}, \tag{3.7}$$

where $C_{IJ} = -(q^{(I)} - q^{(J)})^{-1} Q_1^{(IJ)}$ for $I \neq J$, and

$$\tilde{F}_L^{\prime(J)} = C_{JJ} \tilde{F}_L^{(J)} + \tilde{D}_L^{(J)} \tag{3.8}$$

where $\tilde{D}_L^{(J)} = \sum_{I \neq J} C_{IJ} \tilde{F}_L^{(I)}$, $C_{JJ} = -\tilde{D}_L^{(J)} \tilde{F}_L^{(J)}$. The above formulae are true for all eigenvalues and eigenvectors (for r different from the cutoff values).

Using these formulae we find the radius of curvature $R(r)$ (at two points of the slowness curve), and $\tilde{F}_K^{\bullet(\pm)}(s^{\pm}) = \tilde{F}_K^{\prime(\pm)}(r)/s^{\prime\pm}(r)$. The next step consists in finding the limits of these quantities, and of $\tilde{F}_K^{(\pm)}(r)$, for $r \to r_c$, i.e. $R_c = R(r_c)$, $\tilde{F}_K^{\bullet(0)}$, and $\tilde{F}_K^{(0)}$. In numerical calculations, this simply means finding the values of the quantities for r reasonably close to r_c.

Inserting the eigenvector given by Eq. (3.2) into Eq. (2.7) we get the approximated matrix

$$Z_{KL}^{\pm}(r) = Z_{KL}^{\pm(0)} \pm Z_{KL}^{\pm(1)} \alpha\rho(r) \tag{3.9}$$

(the higher-order terms are neglected) where the constant matrices $Z_{KL}^{\pm(0)}$ and $Z_{KL}^{\pm(1)}$ can be easily expressed in terms of $\tilde{F}_K^{(0)}$, $\tilde{F}_K^{\bullet(0)}$, and the remaining six eigenvectors for $r = r_c$ (see Appendix). In particular,

$$Z(r) = Z_0 - Z_1 \alpha\rho(r), \tag{3.10}$$

where the coefficients Z_0 and Z_1 are the elements (4,4) of the corresponding matrices in Eq. (3.9).

The above formula is true in a close neighborhood of r_c. To take into account the Rayleigh singularity it should be replaced by

$$Z(r) = Z_0 \frac{1 - c_z\rho(r)}{1 - c_i\rho(r)} \tag{3.11}$$

with $c_i = 1/\rho(r_i)$, $c_z = 1/\rho(r_z)$, where r_i is the singular point and r_z is the zero point of $Z(r)$. The coefficients c_i and c_z satisfy the relation

$$c_i - c_z = \alpha Z_1 / Z_0 \,, \tag{3.12}$$

so that only one can be exact. In all the examples presented in Fig. 3 to Fig. 6 we have chosen the coefficient c_i to be exact; the other one is calculated from Eq. (3.12). In this way, the function $Z(r)$ given by Eq. (3.11) is singular for $r = r_i$ (as the exact function $Z(r)$), equal to zero for $r = r_z$ (where r_z is close to the zero point of the exact function $Z(r)$), and its first derivative is infinite for $r = r_c$ (as the first derivative of the exact function $Z(r)$).

Alternatively, we may choose the coefficient c_z to be exact, and calculate the other one from Eq. (3.12). The choice depends on what is considered to be the Green function in view of Eq. (2.8): the Fourier transform of $Z(r)$ or of $Y(r) = 1/Z(r)$. Moreover, we may choose both c_i and c_z to be exact, and calculate from Eq. (3.12) the coefficient Z_1. In this case, the approximation of $Z(r)$ in the neighborhood of r_c is a bit worse but for $r = r_c$ its main features remain unchanged: $Z = Z_0$ and the first derivative of Z is infinite.

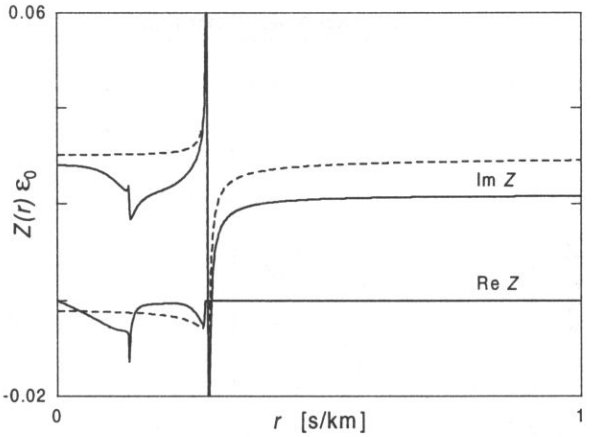

Fig. 3. The function $Z(r)$ (exact: *solid curve*, approximated: *dashed curve*) for lithium niobate (Euler angles: 0°, 90°, 90°).

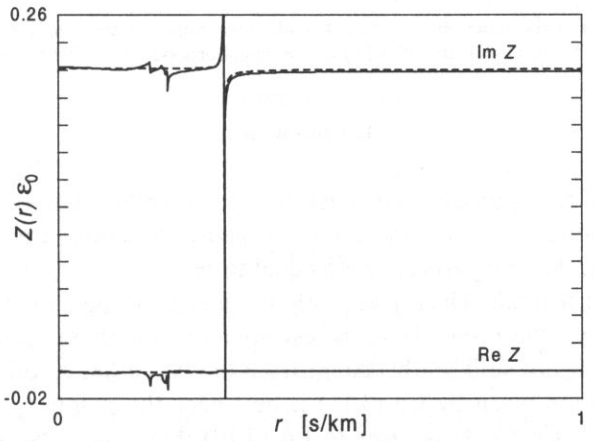

Fig. 4. The function $Z(r)$ (exact: *solid curve*, approximated: *dashed curve*) for quartz (Euler angles: 0°, 90°, 0°).

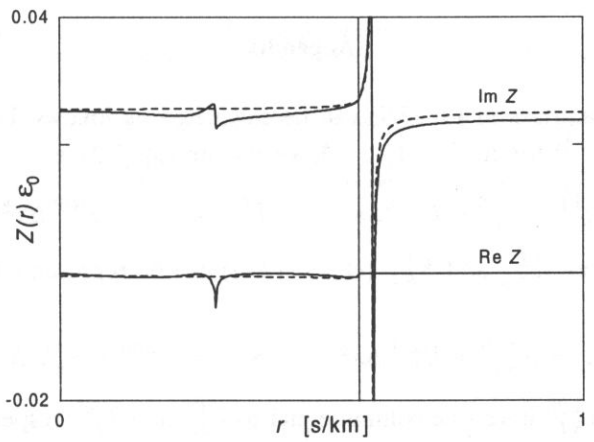

Fig. 5. The function $Z(r)$ (exact: *solid curve*, approximated: *dashed curve*) for bismuth germanium oxide (Euler angles: 0°, 0°, 45°). The vertical line marks r_c.

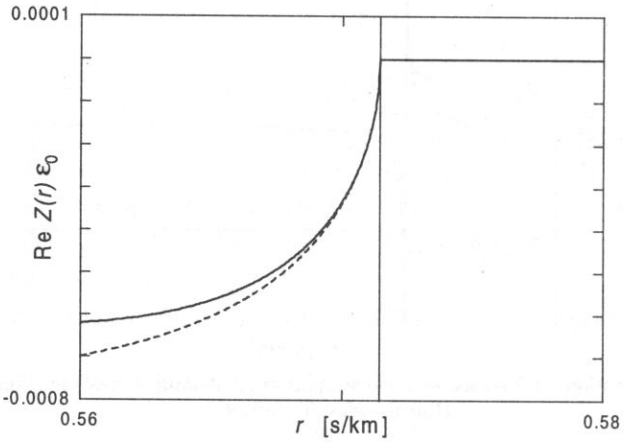

Fig. 6. The real part of the function $Z(r)$ (exact: *solid curve*, approximated: *dashed curve*) for bismuth germanium oxide (Euler angles: 0°, 0°, 45°) in the neighborhood of r_c. The vertical line marks r_c.

4. Conclusion

The behavior of the approximated function $Z(r)$ resembles that of the exact function $Z(r)$ in the whole range of r, and the values of the two functions are quite close to each other. In particular, the real parts are both equal to zero for $r > r_c$ (this feature is absent in the Ingebrigtsen formula which gives only the imaginary part of $Z(r)$). It should be added, however, that the resemblance is less apparent for those crystal cuts for which the cutoff point r_c is not sufficiently distant from the two other cutoff points.

The approximation given by Eq. (3.11) is best near the points r_c, r_i, and r_z. In the neighborhood of r_c, Eq. (3.11) reduces to Eq. (3.10). For $r = r_c$ both the real and the imaginary part of the first derivative of $Z(r)$ have a square-root singularity.

Appendix

The constant matrices in Eq. (3.9) can be calculated as follows. Using the notation $(\tilde{F}_J^{(\pm)}) = (\tilde{U}_K^{(\pm)}, \tilde{T}_L^{(\pm)})$ for $K, L = 1, \ldots, 4$, we rewrite Eq. (3.2) as

$$\tilde{U}_K^{(\pm)} = \tilde{U}_K^{(0)} + \tilde{U}_K^{\bullet(0)} \Delta s^{\pm}, \qquad \tilde{T}_L^{(\pm)} = \tilde{T}_L^{(0)} + \tilde{T}_L^{\bullet(0)} \Delta s^{\pm}. \tag{A.1}$$

Each of the matrices $R_{KL}^{\pm}$ and $S_{KL}^{\pm}$ (cf. Eq. (2.4)) can be represented as a sum of two matrices. We have

$$R_{KL}^{\pm} = R_{KL}^{\pm(0)} + R_{KL}^{\pm(1)} \Delta s^{\pm}, \qquad S_{KL}^{\pm} = S_{KL}^{\pm(0)} + S_{KL}^{\pm(1)} \Delta s^{\pm}, \tag{A.2}$$

where $R_{KL}^{\pm(0)}$ and $S_{KL}^{\pm(0)}$ have one column equal to $\tilde{U}_K^{(0)}$ and $\tilde{T}_L^{(0)}$, respectively, and $R_{KL}^{\pm(1)}$ and $S_{KL}^{\pm(1)}$ have all elements equal to zero except in one column which is equal to $\tilde{U}_K^{\bullet(0)}$ and $\tilde{T}_L^{\bullet(0)}$, respectively.

The matrix $L^{\pm}_{KL}$ is the inverse of the matrix $S^{\pm}_{KL}$. If we put

$$L^{\pm}_{KL} = L^{\pm(0)}_{KL} + L^{\pm(1)}_{KL}\Delta s^{\pm} \tag{A.3}$$

where $L^{\pm(0)}_{KL}$ is the inverse of $S^{\pm(0)}_{KL}$, then

$$S^{\pm}_{KI}L^{\pm}_{IL} = I_{KL} + (S^{\pm(0)}_{KI}L^{\pm(1)}_{IL} + S^{\pm(1)}_{KI}L^{\pm(0)}_{IL})\Delta s^{\pm}, \tag{A.4}$$

(the higher order terms are neglected), and hence,

$$L^{\pm(1)}_{KL} = -L^{\pm(0)}_{KI}S^{\pm(1)}_{IJ}L^{\pm(0)}_{JL} \tag{A.5}$$

for $I, J = 1, \ldots, 4$. Inserting $R^{\pm}_{KL}$ and $L^{\pm}_{KL}$ into Eq. (2.7), and neglecting the higher order terms, we get Eq. (3.9) with

$$Z^{\pm(0)}_{KL} = R^{\pm(0)}_{KI}L^{\pm(0)}_{IL}, \qquad Z^{\pm(1)}_{KL} = R^{\pm(0)}_{KI}L^{\pm(1)}_{IL} + R^{\pm(1)}_{KI}L^{\pm(0)}_{IL}. \tag{A.6}$$

Acknowledgement

This work was supported by Committee of Scientific Research, Poland.

References

[1] K.A. INGEBRIGTSEN, *Surface waves in piezoelectrics*, J. Appl. Phys., **40**, 2681–2686 (1969).

[2] K. BLØTEKJAER, K.A. INGEBRIGTSEN and H. SKEIE, *A method for analyzing waves in structures consisting of metal strips on dispersive media*, IEEE Trans. Electron Devices, **ED-20**, 1133–1138 (1973).

[3] E. DANICKI, *New theory of SSBW devices*, [in:] 1980 IEEE Ultrasonics Symposium Proceedings, B.R. MCAVOY [Ed.] (IEEE, New York, 1980), pp. 235–239.

[4] E.L. ADLER, *SAW and pseudo-SAW properties using matrix methods*, IEEE Trans. UFFC, **41**, 699–705 (1994).

[5] E. DANICKI and W. LAPRUS, *Piezoelectric interfacial waves in langasite and dilithium tetraborate*, [in:] 1995 IEEE Ultrasonics Symposium Proceedings, M. LEVY, S.C. SCHNEIDER and B.R. MCAVOY [Eds.] (IEEE, New York, 1995), pp. 1011–1014.

[6] E. DANICKI and W. LAPRUS, *Piezoelectric interfacial waves in langasite and dilithium tetraborate*, Arch. Acoust., **21**, 99–107 (1996).

[7] W. LAPRUS and E. DANICKI, *Piezoelectric interfacial waves in lithium niobate and other crystals*, J. Appl. Phys., **81**, 855–861 (1997).